A&A manuscript no.
(will be inserted by hand later)

Your thesaurus codes are:
08 (03.13.2; 08.02.3; 08.09.2 (Cyg X-1); 13.25.3)

ASTRONOMY AND ASTROPHYSICS

Frequency resolved spectroscopy of Cyg X-1: fast variability of the Fe K_α line.

M. Revnivtsev[1,2], M. Gilfanov[2,1], E. Churazov[2,1]

[1] Space Research Institute, Russian Academy of Sciences, Profsoyuznaya 84/32, 117810 Moscow, Russia,
[2] Max-Planck-Institute für Astrophysik, Karl-Schwarzschild-Str. 1, 85740 Garching bei München, Germany

Abstract. We studied the frequency resolved energy spectra of Cyg X–1 during the standard low (hard) spectral state using the data of the Rossi X-Ray Timing Explorer. We found that the relative amplitude of the reflection features – the iron fluorescent line at ~ 6.5 keV and the smeared edge above ~ 7 keV – decreases with the increasing frequency. In particular we found that the equivalent width of the iron line decreases above ~ 1 Hz and drops twice at frequency of ~ 10 Hz.

An assumption that such behavior is solely due to a finite light crossing time of the reflecting media, would imply the characteristic size of the reflector $\sim 5\times10^8$ cm, corresponding to $\sim 150R_{\rm g}$ for a $10M_\odot$ black hole. Alternatively lack of high frequency oscillations of the reflected component may indicate that the short time scale, ~ 50–100 msec, variations of the primary continuum appear in geometrically different, likely inner, part of the accretion flow and give a rise to a significantly weaker, if any, reflected emission than the longer time scale events.

Key words: Methods: data analysis – Stars: binaries: general – Stars: individual:(Cyg X-1) – X-rays: general

1. Introduction

Over the last several years it has become widely accepted that the Galactic X-ray binaries exhibit Compton reflection features in their spectra.

Qualitatively, the reflection component in the X-ray spectra of these systems can be described as a broad "hump" at energies 20–30 keV, fluorescent Fe line at energies 6.4–6.7 keV (depending on the ionization state of the reflecting medium) and an absorption edge at the energy $\approx$7.1 keV (Basko, Sunyaev & Titarchuk, 1974, George & Fabian, 1991). For all geometries which do not obscure the direct primary continuum from the observer, the detected energy spectra consists of this direct component (approximately a power law in the 3–13 keV energy band) and the reflection features. For standard cosmic abundances the expected equivalent width of the fluorescent Fe line is $\sim$100–200 eV (for a source above semi–infinite slab of neutral matter).

The geometry and mutual location of the source of primary continuum and reflecting medium should affect both the equivalent width of the fluorescent line and the character of it's variability. In particular the finite size of the reflector implies that the time variations of the reflected radiation should be smeared out on the time scales corresponding to the light crossing time of the reflector. In addition, a time lags between different emission components might apprear. Alternatively the geometrically different region of the main energy release zone (where the primary continuum is produced) may have different efficiency for production of the reflection component. As a result timing properties of the reprocessed component may be linked to the properties of the selected region of this zone.

2. Observations and data analysis

For our analysis we chose publicly available data of the Rossi X-ray Timing Explorer observations P10238 performed between Mar. 26, 1996 and Mar. 31, 1996 with a total exposure time $\sim$70 ksec (we used only observations were all 5 PCU were turned on). For the frequency resolved spectral analysis we used PCA data in the "Generic Binned" mode, having $\frac{1}{64}$sec$\sim$16 msec time resolution in 64 energy channels covering the whole PCA energy band (B_16ms_64M_0_249). For analysis of the averaged spectrum we used the "Standard Mode 2" data, having twice as many energy channels in the energy band of our interest (3–13 keV) than the "Generic Binned" mode.

For the obtained spectra we constructed the response matrix using the standard tasks of FTOOLS 4.2 package with PCA RMF v3.5 (Jahoda 1999). The comparison of the timing mode spectra with that obtained from "Standard Mode 2" showed, that they do not differ more than

Send offprint requests to: revnivtsev@hea.iki.rssi.ru

by 1–1.5%. The background was calculated using "Q6" model (VLE-based model, preferable for bright sources does not work for these observations). However, the PCA background is negligible for the time averaged spectra of Cyg X-1 in the energy band 3–13 keV. The PCA background contribution to the frequency resolved spectra at the frequencies 0.03–30 Hz is even less important.

3. Frequency resolved spectral analysis

We calculated the Power Density Spectra (PDSs) in each energy channel for every 128 sec time segments using the standard Fast Fourier Transform (FFT) procedure and adopting the normalization of Miyamoto et al. (1991):

$$P_j = 2|a_j|^2/N_\gamma R$$

$$a_j = \sum_{k=1}^{2^m} x_k e^{i\omega_j t_k}$$

where t_k is the time label of the kth bin, x_k is the number of counts in this bin, N_γ is the total number of photons and R is the average count rate in the segment ($R = N_\gamma/T$, T – total duration of the light curve segment). This PDS normalization ((rms/mean)^2/Hz) allows one to obtain squared fractional rms by integrating the power over the frequencies of interest. Then the obtained power spectra were averaged over the light curve segments and the logarithmic frequency bins. For every obtained frequency bin the frequency dependent spectra were constructed according to the formula:

$$S(E_i, f_j) = R_i\sqrt{P_i(f_j)\Delta f_j} = \sqrt{\frac{2|a_{ij}|^2}{T}\Delta f_j}$$

here $S(E_i, f_j)$ is the count rate of the spectrum on the frequency f_j in the energy channel E_i. Since the light curves of Cyg X-1 in the different energy bands almost perfectly coherent and have practically the same form of the PDS (see e.g. Nowak et al. 1999), the spectra obtained using the procedure above can be used to describe the real energy spectrum of the source X-ray flux variations on the different time scales. The above expession also can be easily adapted to describe the energy spectrum of different PDS spectrum components.

4. Results

The energy spectra of Cyg X–1 in several narrow frequency ranges between 0.03 and 30 Hz are shown in Fig. 1. The change of the spectral shape with the decrease of the characteristic time scale can be clearly seen. The relative amplitude of the reflection features, in particular that of the broad line at $\sim$ 6–7 keV and the "smeared edge" above

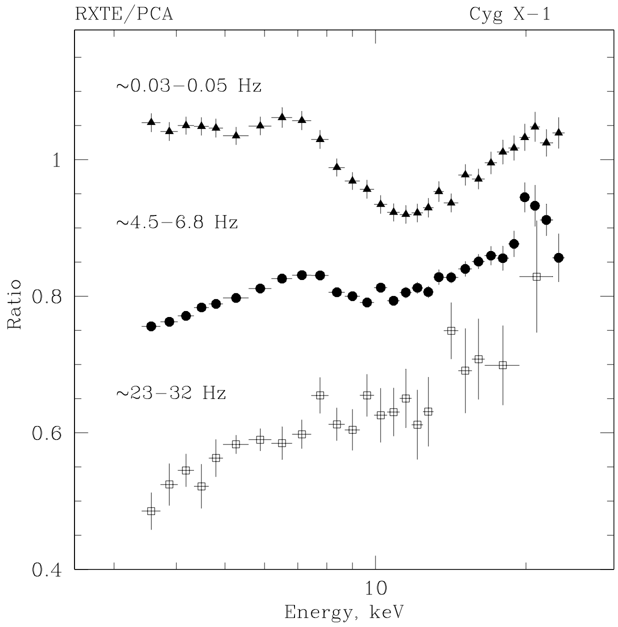

Fig. 1. The ratio of the energy spectra of Cyg X-1 in different frequency bands to a power law model with photon index $\alpha = 1.8$. Spectra corresponding to 0.03-0.05 Hz and 23–32 Hz were rescaled for clarity.

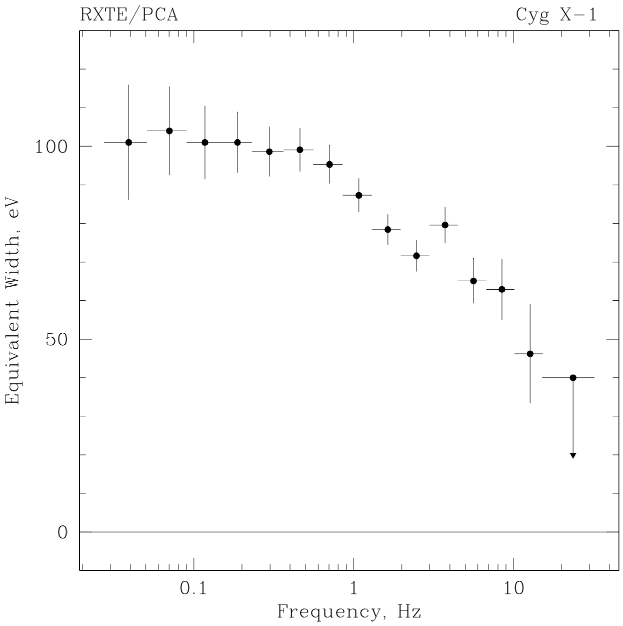

Fig. 2. Dependence of the equivalent width of the fluorescent Fe line on the frequency. For the spectral approximation the powerlaw+gaussian line model was used (3–13 keV energy band, the centroid energy and the width of the line were frozen at the values 6.4 keV and 0.1 keV respectively).

Table 1. Best fit parameters of the approximation of frequency dependent spectra of Cyg X-1 with the power law + gaussian line (line energy and width were frozen at the values 6.4 keV and 0.1 keV respectively) in the energy band 3–13 keV.

Freq., Hz	PL slope,α	EW, eV
$(3.9 \pm 1.2) \times 10^{-2}$	1.93 ± 0.01	101 ± 15
$(7.0 \pm 1.9) \times 10^{-2}$	1.91 ± 0.01	104 ± 12
0.12 ± 0.03	1.91 ± 0.01	101 ± 9
0.19 ± 0.04	1.89 ± 0.01	101 ± 8
0.30 ± 0.07	1.89 ± 0.01	98.6 ± 6.4
0.46 ± 0.09	1.89 ± 0.01	99.1 ± 5.6
0.7 ± 0.14	1.89 ± 0.01	95.3 ± 4.9
1.07 ± 0.22	1.86 ± 0.01	87.3 ± 4.4
1.63 ± 0.33	1.83 ± 0.01	78.4 ± 3.9
2.48 ± 0.50	1.81 ± 0.01	71.6 ± 4.0
3.74 ± 0.76	1.80 ± 0.01	79.6 ± 4.7
5.63 ± 1.14	1.75 ± 0.01	65.1 ± 5.8
8.48 ± 1.71	1.70 ± 0.01	62.9 ± 7.9
12.7 ± 2.6	1.63 ± 0.01	46.2 ± 12.8
19.2 ± 3.8	1.62 ± 0.01	$< 48^a$
27.5 ± 4.5	1.63 ± 0.01	$< 57^a$

[a] – 2σ upper limit

~ 7 keV, is apparently decreasing with the increase of frequency and vanishes above ~ 20 Hz. Along with becoming less "wiggled" the spectra become harder as frequency increases.

In order to quantify these effects we fit frequency resolved spectra in 16 frequency bins covering 0.03–32 Hz range in the 3–13 keV energy band with a simple two component model consisting of a power law and a Gaussian line with the fixed energy $E_{\rm line} = 6.4$ keV and the width FWHM=0.1 keV (that is comparable with the PCA energy resolution at this energy). The best fit parameters are given in Table 1. The dependence of the line equivalent width upon frequency is shown in Fig. 2. As is seen from the Fig. 2, the equivalent width of the line starts decreasing above ~ 1 Hz and falls by a factor of 2 at ~ 10 Hz. No significant flux in the line was detected above 15 Hz with the 2σ upper limit on the equivalent width in the 15–32 Hz frequency range of $\approx$40 eV.

Variations of the parameters of the spectral model, in particular the change of the line centroid to 6.0 and 6.7 keV and increase of the line width to 1.0 keV, do not change the general trend. These variations, however, affect the particular values of the equivalent width and, to some extent, the shape of the curve in Fig. 2. The change of the line centroid energy to the 5 keV or 9 keV, on the contrary, results in disappearance of the effect.

Finally we should mention that similar behaviour of the frequency resolved spectra was detected in Cyg X-1 observations 20175-01-01-00, 20175-01-02-00 and in all available observations of the set P30157 (01–10), performed in 1997 but with lower significance.

5. Discussion

A time averaged energy spectrum of Cyg X-1 (e.g. Ebisawa et al. 1992, Gierlinski et al. 1997) as well as frequency resolved spectra at low frequency (Fig.1) show clear deviation from a single slope power law spectrum. This deviation is commonly ascribed to the reflection from an optically thick media located in the vicinity of the production site of primary hard X–ray radiation. In a simple case of reflection from an optically thick cold neutral medium the main reflection features are well known (Basko, Sunyaev & Titarchuk, 1974, George & Fabian, 1991) – a narrow unshifted iron K_α line at 6.4 keV with an equivalent width of ~ 100 eV, an absorption edge at ≈ 7.1 keV and a reflected continuum peaked at $\sim 20 - 30$ keV. However, the real spectra of compact X–ray binaries show considerably more complicated behavior. In particular the centroid energy of the line is often different from 6.4 keV, the line width in many cases is as large as ~ 1 keV and a broad "smeared edge" above $\sim$ 7–8 keV is observed instead of a sharp absorption edge at ≈ 7.1 keV (Ebisawa et al. 1992). This departure from a simple reflection model hints at a complicated ionization state and/or motion (e.g. Keplerian motion in the disk) of the reflecting media.

It is obvious, that the simple spectral model used for fitting the data in the previous section is neither adequate nor completely justified from the physical point of view. The apparent line centroid energy and width vary with frequency. In particular the best fit centroid energy shifts below 6.0 keV and the width of the line exceeds 1 keV as frequency increases. However, due to the lack of a satisfactory realistic model of reflection in an X–ray binary, especially applicable to the frequency resolved spectral data, we restricted ourselves to the simple two component model described in the previous section. The main purpose of using this spectral model was to quantify the major effect which is clearly seen in Fig.1, namely the suppression of the reflection features in the energy spectrum with the increase of frequency.

The results of the analysis presented in this paper show that the relative amplitude of the reflected component variations is lower on the short time scales ($\lesssim$ 50–100 msec), than that of the primary X-ray radiation. Similar effect was found Oosterbroek et al. (1996) for GS 2023+338 but the characteristic time scale in this case was much longer, $\sim$200 sec. GS 2023+338 is peculiar in many ways. In particular the source exhibited strong ($\gtrsim 10^{23}$ cm^{-2}) and highly variable on the time scales of $\sim 10^3$ sec low energy absorption (e.g. Zycki, Done & Smith 1999) and, most importantly, extremely strong Fe line with equivalent width up to 1.4 keV (Oosterbroek et al. 1996), that could mean that geometry of the reprocessing media in GS2023+338 is different from that in Cyg X–1. Recently we found suppression of the reflected component variations in the low spectral state of another black hole candidate GX339–4 (Revnivtsev, Gilfanov & Churazov, 1999). In this case the characteristic time scale (∼50–100 msec) was similar to that in Cyg X–1. We therefore can tentatively conclude that such a behavior might be a common feature of the black hole binaries in the low spectral state.

A most straightforward explanation of this effect would be in terms of a finite light crossing time of the reflector $\tau_{\rm refl} \sim l_{\rm refl}/c$, caused by a finite spatial extend $l_{\rm refl}$ of the reflecting media. From Fig.2 one can see that the equivalent width of the iron line drops by a factor of two at the frequency $f_{1/2} \sim 10$ Hz. This value gives us a rough estimate of the characteristic response time of the reflector $\tau_{\rm refl} \sim 1/2\pi f_{1/2} \sim 15$ msec and the characteristic size of the reflecting media $l_{\rm refl} \sim 5\times10^8$ cm which would correspond to $\sim 150R_{\rm g}$ for a $10M_{\odot}$ black hole. We note however that if the primary continuum originates within the $\sim 10R_{\rm g}$ sphere in the inner zone of the accretion disk, then only a small fraction of the emitted hard radiation has the possibility to be reflected from the accretion disk regions with $R \gtrsim 150R_{\rm g}$ (in the case of a flat disk) and it can hardly provide observed ~ 100 eV equivalent width of the iron line. Therefore the assumption that high frequency variations of the reflected component are caused by the finite light crossing time of the reflector implies interesting constraints on the geometry of the source of primary continuum and reflector.

An alternative explanation might be that the short time scale, $\lesssim$ 50–100 msec, variations appear in geometrically different, likely inner, part of the accretion flow and give a rise to significantly weaker, if any, reflected emission than the longer time scale events, presumably originating in the outer regions. This might be caused, for instance, by a smaller solid angle of the reflector as seen by the short time scale events and/or due to screening of the reflector from the short time scale events by the outer parts of the accretion flow.

Acknowledgements. This research has made use of data obtained through the High Energy Astrophysics Science Archive Research Center Online Service, provided by the NASA/Goddard Space Flight Center.

References

Basko M., Sunyaev R. & Titarchuk L., 1974, A&A, 31, 249
Ebisawa K., Inoue H., Mitsuda K., Nagase F., Tanaka Y., Yaqoob T., Yoshida K., 1992, in Frontiers of X-ray Astronomy, ed. Y. Tanaka & K. Koyama (Tokyo: University Press), 301
George I.M., Fabian A.C., 1991, MNRAS, 249, 352
Gierlinski M., Zdziarski A., Done C., Johnson W., Ebisawa K., Ueda Y., Haardt F., Phlips B., 1997, MNRAS, 288, 958
Miyamoto S., Kimura K., Kitamoto S., Dotani T., Ebisawa K., 1991, ApJ, 383, 784
Nowak M., Vaughan B., Wilms J., Dove J., Begelman M., 1999, ApJ, 510, 874
Oosterbroek T., van der Klis M., Vaughan B., van Paradijs J., Rutledge R., Lewin W.H.G., Tanaka Y., Nagase F., Dotani T., Mitsuda K., Yoshida K. 1996, A&A, 309, 781
Revnivtsev M., Gilfanov M., Churazov E. 1999, in preparation
Stark M., 1999, http://lheawww.gsfc.nasa.gov/∼stark/pca/pcabackest.html
Jahoda K., 1999, http://lheawww.gsfc.nasa.gov/users/keith/pcarmf.html
Zycki P., Done C., Smith D. 1999, MNRAS, 305, 231